Nanoparticle engineered TRAIL-overexpressing adipose-derived stem cells target and eradicate glioblastoma via intracranial delivery

Xinyi Jiang[a], Sergio Fitch[b], Christine Wang[b], Christy Wilson[c], Jianfeng Li[a], Gerald A. Grant[c], and Fan Yang[a,b,1]

[a]Department of Orthopaedic Surgery, Stanford University, Stanford, CA 94305; [b]Department of Bioengineering, Stanford University, Stanford, CA 94305; and [c]Department of Neurosurgery, Stanford University, Stanford, CA 94305

Edited by Robert Langer, Massachusetts Institute of Technology, Cambridge, MA, and approved October 17, 2016 (received for review September 29, 2016)

Glioblastoma multiforme (GBM) is one of the most intractable of human cancers, principally because of the highly infiltrative nature of these neoplasms. Tracking and eradicating infiltrating GBM cells and tumor microsatellites is of utmost importance for the treatment of this devastating disease, yet effective strategies remain elusive. Here we report polymeric nanoparticle-engineered human adipose-derived stem cells (hADSCs) overexpressing tumor necrosis factor-related apoptosis-inducing ligand (TRAIL) as drug-delivery vehicles for targeting and eradicating GBM cells in vivo. Our results showed that polymeric nanoparticle-mediated transfection led to robust up-regulation of TRAIL in hADSCs, and that TRAIL-expressing hADSCs induced tumor-specific apoptosis. When transplanted in a mouse intracranial xenograft model of patient-derived glioblastoma cells, hADSCs exhibited long-range directional migration and infiltration toward GBM tumor. Importantly, TRAIL-overexpressing hADSCs inhibited GBM growth, extended survival, and reduced the occurrence of microsatellites. Repetitive injection of TRAIL-overexpressing hADSCs significantly prolonged animal survival compared with single injection of these cells. Taken together, our data suggest that nanoparticle-engineered TRAIL-expressing hADSCs exhibit the therapeutically relevant behavior of "seek-and-destroy" tumortropic migration and could be a promising therapeutic approach to improve the treatment outcomes of patients with malignant brain tumors.

nanoparticle | adipose-derived stem cells | TRAIL | glioblastoma | tumor microsatellites

Glioblastoma multiforme (GBM) is the most common and aggressive subtype of malignant brain tumor. Current state-of-the-art treatment consisting of surgical resection in combination with radiation and chemotherapy for GBM fails to address its highly infiltrative nature, often leaving behind microscopic tumor satellites, which results in tumor recurrence. Therapeutic gene delivery by direct injection of viral vectors into the primary brain tumor or postoperative tumor resection cavity has also largely failed to reach outgrowing tumor micrometastatic nests of glioma cells at sites distant from the main tumor mass as well as infiltrating glioma cells in the adjacent brain. As such, it is imperative to develop novel treatment strategies that focus specifically on targeting and eliminating the disseminated neoplastic burden within the brain.

Human stem cells have shown promise as a drug delivery vehicle for targeting infiltrating brain cancer cells that cannot be removed by surgery. Recent research shows that transplanted human neural stem cells (NSCs; hNSCs) possess remarkable tumortropic migratory capacity in vitro and in vivo; hNSCs have been used for the delivery of cytotoxic and immunomodulatory therapies (1–5) and were recently approved for clinical trials. However, the clinical translational potential of hNSCs may be hindered by ethical concerns associated with their isolation, expansion, and associated immune response (6, 7). Bone marrow-derived human mesenchymal stem cells (hMSCs) exhibit selective tropism similar to hNSCs, migrating significant distances to target gliomas (8). Unlike hNSCs and hMSCs, human adipose tissue-derived stem cells (hADSCs) represent an abundant and easily accessible autologous source of stem cells, with fewer ethical concerns associated with their use. Additionally, unmodified hADSCs remain free of oncogenic transformation for at least 8 mo when injected into immunocompromised mice, demonstrating more oncogenic resistance than human bone marrow-derived stem cells (9). Therefore, hADSCs derived from fat tissue could represent a better alternative for stem cell-based cancer gene therapy.

By using stem cells as drug delivery vehicles, different biological drugs have been delivered, including chemotherapeutic agents, prodrugs (10–13), and genetic signals (14). One limitation of delivering chemotherapeutic agents is that they generally could not differentiate cancerous cells from normal cells. To avoid undesirable cytotoxicity to normal cells, here we have specifically chosen the full length of tumor necrosis factor-related apoptosis-inducing ligand (TRAIL), a type II membrane-bound protein that can rapidly induce apoptosis in a variety of cancers while leaving normal cell types intact. TRAIL induces apoptosis by binding to its death receptors DR4 and DR5, forming a homotrimeric complex (TRAIL-R1/D4 and TRAIL-R2/D5), causing caspase-8 activation in the death-inducing signaling complex; this complex can directly cleave caspase-3 to activate extrinsic pathways or cleave the Bcl-2–inhibitory

Significance

Current treatment for glioblastoma multiforme (GBM) fails to address its highly infiltrative nature; treatment often leaves behind microscopic neoplastic satellites, resulting in eventual tumor recurrence. Here we report polymeric nanoparticle-engineered human adipose-derived stem cells (hADSCs) overexpressing the cancer-specific TNF-related apoptosis-inducing ligand for targeting and eradicating glioblastoma cells. Engineered hADSCs exhibited long-range directional migration toward tumor in patient-derived GBM orthotropic xenografts and showed significant inhibition of tumor growth and extension of animal survival. Repetitive injection further prolonged animal survival compared with single injection. Together, our data suggest that nanoparticle-engineered hADSCs exhibit the therapeutically relevant behavior of "seek-and-destroy" tumortropic migration, and may offer a promising therapy for substantial enhancement of GBM treatment.

Author contributions: X.J., C. Wang, G.A.G., and F.Y. designed research; X.J. and S.F. performed research; C. Wilson contributed new reagents/analytic tools; X.J., S.F., C. Wang, C. Wilson, J.L., G.A.G., and F.Y. analyzed data; and X.J., S.F., G.A.G., and F.Y. wrote the paper.

The authors declare no conflict of interest.

This article is a PNAS Direct Submission.

[1]To whom correspondence should be addressed. Email: fanyang@stanford.edu.

This article contains supporting information online at www.pnas.org/lookup/suppl/doi:10.1073/pnas.1615396113/-/DCSupplemental.

BH3-domain–containing protein to activate the intrinsic pathway (15, 16). A recombinant soluble version of the transmembrane death ligand TRAIL has shown compelling preclinical results as a potential cancer therapeutic agent, but only rare clinical responses have been observed in clinical trials, possibly because of insufficient tumor exposure (17, 18) and/or weak engagement of the extrinsic pathway (19, 20). On the contrary, in the case of viral-mediated TRAIL gene therapy, limitations arise from triggering immune responses and unintended genomic integration events (21, 22), which remain a key bottleneck for broad clinical application.

Here, we sought to develop biodegradable nanoparticle-engineered stem cells to efficiently express the suicide protein TRAIL for targeting and eradicating microsatellites and infiltrating glioma cells in patient-derived adult glioblastoma orthotropic xenograft models. Compared with methods that use nonviral gene therapy alone, this combined polymer/stem cell approach takes advantage of the stem cell's ability to track microsatellites and infiltrating glioma cells. TRAIL secreted on the surface of hADSCs binds the death receptors DR4 and DR5 on tumor cells and triggers tumor cell death. hADSCs were modified with TRAIL DNA via amino group-ended poly(β-amino ester)s (PBAEs), hydrolytically biodegradable polymers that can condense DNA to form nanoparticles. We showed that polymeric nanoparticle-engineered hADSCs led to robust TRAIL up-regulation in hADSCs compared with cells transfected with plasmid control DNA (pCDNA). Patient-derived glioma xenograft cells cocultured with TRAIL-expressing hADSCs exhibited significant cell death 48 h after exposure. In vivo, GBM xenograft mice treated with nanoparticle-engineered TRAIL-expressing hADSCs significantly inhibited tumor growth in mice and substantially prolonged animal survival compared with hADSCs modified with pCDNA-laden nanoparticles, naïve hADSCs, or PBS solution. Repetitive injection of TRAIL-overexpressing hADSCs significantly prolonged animal survival compared with single injection of those cells. Together, our results suggest that nanoparticle-engineered hADSCs could serve as cellular vehicles for targeting and eradicating GBM cells in a smart "seek-and-destroy" fashion, thereby improving the treatment outcomes of this devastating disease.

Results

Biodegradable Nanoparticle-Mediated hADSCs Transfection in Vitro. Primary hADSCs are relatively resistant to transfection with nonviral methods. Using a leading commercially available transfection reagent (Lipofectamine 2000), the highest transfection efficiency we achieved was ∼7.37 ± 0.96%, which is far from sufficient to achieve therapeutic efficacy for clinical application. Based on our recent work on biodegradable nanoparticle-mediated transfection in stem cells (23, 24), we further systematically optimized the nanoparticle-fabrication formulation and the transfection protocol with our custom-developed amino group end-modified PBAEs. As shown via agarose gel electrophoresis, the DNA plasmid was completely condensed in polymer nanoparticles when the weight ratio of polymer and plasmid coded with recombinant enhanced GFP (pEGFP) in nanoparticles was greater than 10:1 (Fig. S1*A*). For a deep investigation of the biochemophysical properties of PBAE nanoparticles, we systemically measured the particle size and zeta potential of nanoparticles with different formulations. Along with the increase of polymer ratio, the size of the nanoparticles significantly decreased as shown in a dynamic light scattering assay, and, because of the binding of proteins in the serum, the particles showed increased size in full supplemented Dulbecco's modified Eagle medium containing 10% (vol/vol) FBS compared with that in deionized water (Fig. S1*B*). Nanoparticles suspended in deionized water have a positive charge, whereas the surface charge of nanoparticles becomes slightly negative when suspended in cell-culture medium (Fig. S1*C*). Using GFP as a reporter gene, we further titrated the nanoparticle-mediated transfection formulation by using hADSCs. By using a leading nanoparticle formulation with a weight ratio of polymer to pEGFP of 20:1, we achieved ∼5.48-fold higher transfection efficiency in hADSCs vs. a control group transfected using Lipofectamine 2000 (Fig. S2). Dynamic light scattering analysis showed the leading PBAE nanoparticles in deionized water have a Z-average diameter of ∼183.6 nm (Fig. 1*A*) and a zeta potential of ∼40.06 mV (Fig. 1*B*), and transmission electron microscope (TEM) revealed that the nanoparticles exhibited a spherical shape (Fig. 1*C* and Fig. S3).

Biodegradable Nanoparticle-Mediated Transfection Induced Membrane TRAIL Expression by hADSCs in Vitro. Next, we transfected hADSCs with the plasmid vector encoding the native full-length TRAIL (pTRAIL) using the leading PBAE nanoparticles. Forty-eight hours after transfection, hADSCs were harvested for assays of TRAIL expression. Flow cytometry indicated that 68.41 ± 2.65% of nanoparticle-transfected hADSCs expressed TRAIL (Fig. 1*D*). Gene expression analysis via quantitative real-time PCR (qRT-PCR) revealed a 546.07-fold increase in TRAIL expression after transfection with nanoparticles (Fig. 1*E*). Immunoblotting of lysates prepared from cells harvested 48 h after nanoparticle transfection indicated that hADSCs produce TRAIL protein (Fig. 1*F*). Immunostaining showed a strong fluorescence signal from TRAIL antibody in phTAIL-laden nanoparticle-transfected hADSCs, whereas pCDNA-laden nanoparticle-transfected hADSCs

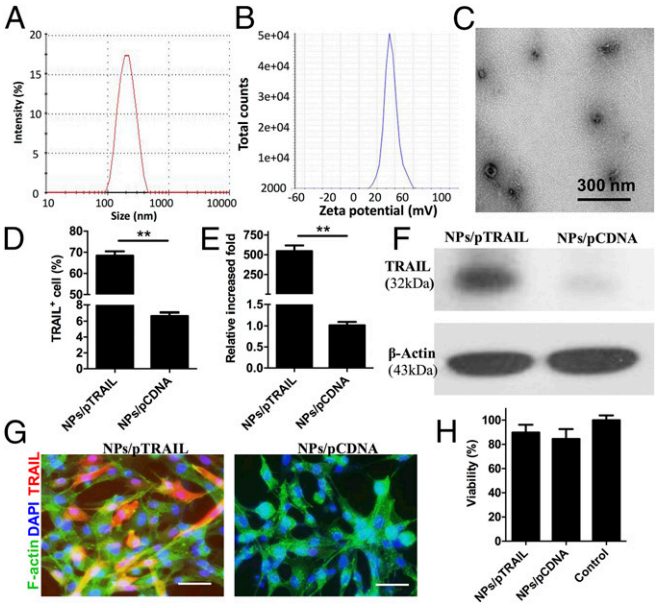

Fig. 1. Polymeric nanoparticles containing TRAIL plasmid DNA led to robust up-regulation of TRAIL in hADSCs. (*A*–*C*) Physicochemical characterization of pEGFP-laden PBAE nanoparticles with a PBAE:pEGFP weight ratio of 20:1. Size distribution (*A*) and zeta potential (*B*) of nanoparticles determined by dynamic light scattering. (*C*) TEM imaging confirmed that PBAE polymer condensed DNA-forming nanoparticles. (*D*) Flow cytometry analysis of $TRAIL^+$ cell percentage (**$P < 0.01$) and (*E*) qRT-PCR reveals the fold increase of TRAIL mRNA expression in hADSCs vs. GAPDH mRNA expression 48 h after transfection with optimized pTRAIL-laden PBAE nanoparticles (i.e., NPs/pTRAIL; **$P < 0.01$). (*F*) Western blot assay of TRAIL protein expression in hADSCs transfected with NPs/pTRAIL or pCDNA-laden PBAE nanoparticles (i.e., NPs/pCDNA). (*G*) Immunostaining confirmed TRAIL expression in hADSCs; hADSCs transfected with NPs/pCDNA showed minimal TRAIL signals. Red indicates TRAIL, green indicates F-actin, blue indicates cell nucleus. (Scale bars: 10 μm.) (*H*) The viability of cells was analyzed via the MTS assay 48 h after transfection with NPs/pTRAIL. hADSCs transfected with NPs/pTRAIL exhibited no change in viability compared with naïve controls and those transfected with NPs/pCDNA. Untransfected, unmanipulated parallel cultures of hADSCs represented 100% viability.

displayed no fluorescence (Fig. 1*G*). It has been reported that infected cells can secrete TRAIL as a soluble protein into the culture medium, which can be monitored via ELISA (25). However, we did not detect soluble TRAIL in culture medium from nanoparticle-transfected hADSCs. These results demonstrate that all TRAIL expressed in hADSCs was membrane-bound. To determine the cytotoxicity of nanoparticle-induced TRAIL expression in hADSCs, we performed a cellTiter 96 AQueous one solution cell proliferation assay (MTS); there was no significant change in viability in nanoparticle-treated hADSCs vs. naïve hADSCs (Fig. 1*H*).

TRAIL Induces Apoptosis in Glioma Cells but Not in hADSCs and Normal Astrocytes. To test the specificity of TRAIL cytotoxicity against glioma cells and hADSCs, we performed TUNEL immunostaining on cells transfected with phTRAIL nanoparticles. We detected a significant decrease in the viability of GBM cells, whereas hADSCs did not exhibit decreased viability 48 h after transfection (Fig. S4).

Next, we cocultured plasmid human TRAIL-laden nanoparticles (NPs/pTRAIL)-engineered hADSCs with patient-derived malignant glioma xenograft cells (D-270 MG) for 48 h. This coculture resulted in significant apoptosis and death in glioma cells (Fig. 2 *A* and *B*), whereas glioma cells cocultured with hADSCs transfected with plasmid control DNA-laden nanoparticles (NPs/pCDNA) did not demonstrate significant apoptotic activity (Fig. 2 *A* and *B*). The caspases are a family of closely related enzymes crucial to TRAIL-induced apoptosis. zVADfmk is a cell-permeable pan-caspase inhibitor. Application of this compound to 10:1 cocultured glioma cells and hADSCs caused an obvious reduction in death and apoptosis, confirming the importance of caspase pathways in the mechanism of TRAIL-induced glioma cell death (Fig. 2 *A* and *B*).

To confirm that the glioma cell population was responsible for the dead and apoptotic populations, the GBM cells were labeled with the fluorescent dye Dil before the annexin-V apoptosis assay. Our data showed that the apoptotic and dead cells came specifically from the glioma cell population, and that 35.7 ± 4.3% of the glioma cell population was dead or apoptotic, compared with only 4.2 ± 0.6% of the hADSCs population ($P < 0.001$; Fig. 3 *A* and *C*). Normal astrocytes were used as a negative control to verify the cytotoxic specificity of TRAIL-expressing hADSCs against normal brain cells; coculture with TRAIL-expressing hADSCs did not increase normal astrocyte death and apoptosis (Fig. 3 *B* and *C*).

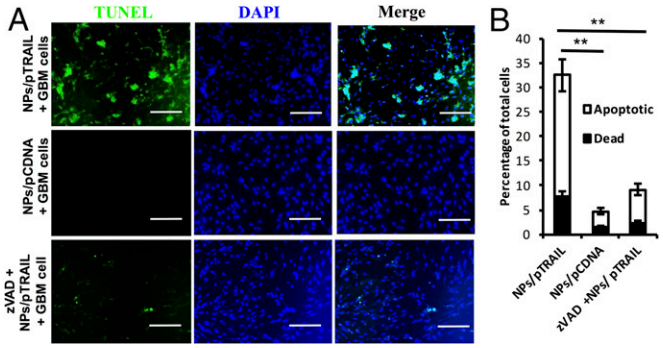

Fig. 2. TRAIL-overexpressing hADSCs induced apoptosis in adult patient-derived glioma xenograft cells in vitro. (*A*) Glioma cells grown in coculture with NPs/pTRAIL-engineered hADSCs exhibited significant cell death 48 h after exposure. These cultures also demonstrated numerous TUNEL$^+$ nuclei, indicating that the majority of cells were undergoing apoptosis (*Top*). In contrast, glioma cell coculture with hADSCs modified with NPs/pCDNA, remained viable (*Middle*). Preincubation with zVADfmk (zvad), a pan-caspase inhibitor, obviously decreased TUNEL$^+$ nuclei (*Bottom*). (Scale bars, 30 μm.) (*B*) Flow cytometry results from triplicate apoptosis assays indicate overall increases in death and apoptosis of total cells in glioma cells and hADSCs grown in coculture (**$P < 0.01$).

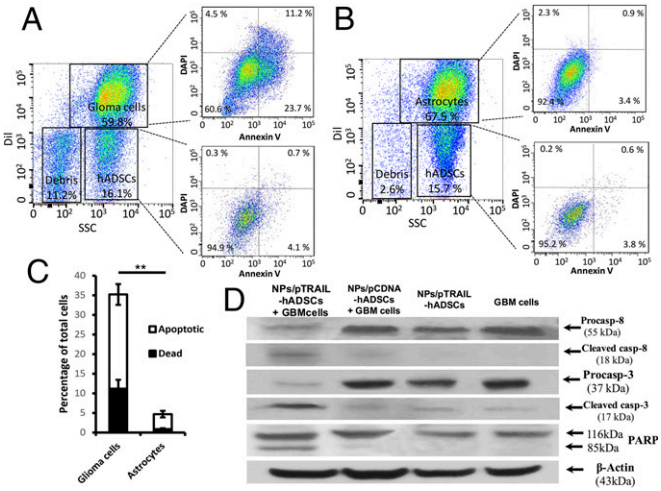

Fig. 3. TRAIL-overexpressing hADSCs selectively induced apoptosis via caspase pathways in GBM cells, but not in normal brain astrocytes in vitro. (*A*–*C*) Dil$^+$ glioma cells were responsible for dead and apoptotic populations. (*A* and *B*) Representative flow cytometry plots reveal an increase in cell death and apoptosis when NPs/pTRAIL-engineered hADSCs were cocultured with glioma cells (*A*) vs. coculture with astrocytes, a normal control (*B*). (*C*) Quantification of flow cytometry (**$P < 0.01$). (*D*) Western blot assay of caspase-8 and caspase-3 activation and cleavage of the caspase substrate proteolytic PARP. Precursors and cleavage products of the caspases and PARP are indicated by arrows. Caspase-8 and caspase-3 activation and PARP cleavage were detected in cocultures of NPs/pTRAIL-engineered hADSCs plus glioma cells, but were nearly absent in cocultures of NPs/pCDNA-engineered hADSCs with glioma cells, NPs/pTRAIL-hADSCs, and glioma cells.

To further demonstrate caspase activation, we examined caspase-8 and caspase-3 activation and cleavage of the caspase substrate proteolytic poly(ADP-ribose) polymerase (PARP) in cell lysis. Coincidental with the annexin V staining data from flow cytometry assay, caspase-8 and caspase-3 activation and PARP cleavage were detected in GBM cells cocultured with NPs/pTRAIL-transfected hADSCs but not in cocultures of NPs/pCDNA-engineered hADSCs with GBM cells, NPs/pTRAIL-hADSCs alone, or GBM cells alone (Fig. 3*D*). These results indicate a rapid activation of caspase-8 and the caspase cascade in TRAIL-induced glioma cell death when GBM cells were cocultured with NPs/pTRAIL-modified hADSCs.

Tropism of Implanted hADSCs Toward Gliomas in Vivo. Next, we investigated whether implanted hADSCs could migrate toward intracranial gliomas through normal brain parenchyma in vivo by using fluorescent-labeled patient-derived GBM xenograft cells (Fig. S5). Unlike immortalized cell lines, these patient-derived GBM cells can better preserve tumor phenotype and predict clinically relevant outcomes (26). Our data showed that patient-derived GBM cells formed microsatellites surrounding main tumor in vivo (Fig. S6), which mimics clinical observations of GBM progression. To compare the effects of delivery routes on the long-range migration ability of hADSCs toward intracranial GBM tumors, Dil-labeled hADSCs were implanted into the hemisphere contralateral to the tumor site or injected via tail vein of the tumor-bearing mice at day 5 after inoculation. Mice were killed 15 d after tumor inoculation, and brain sections were prepared (Fig. 4*A*). Our data showed that Dil-labeled hADSCs inoculated into the hemisphere contralateral to the tumor migrated away from the initial injection site toward the tumor mass along the corpus callosum at 10 d after implantation, whereas hADSCs remained within the injection site in the healthy brain (Fig. 4 *B* and *C*). In

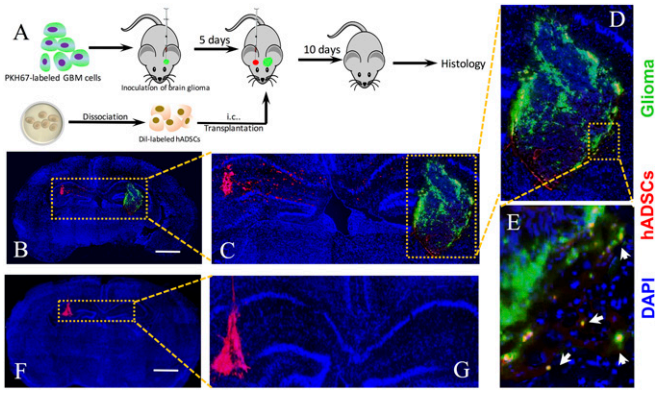

Fig. 4. Human ADSCs exhibited long-range directional migration and infiltration toward GBM tumor in a mouse PDTX model. (*A*) Schematic of experimental design. GBM cells and hADSCs were fluorescently labeled before transplantation in athymic mice. PKH-67-labeled GBM cells (green) were inoculated at day 1. At day 5, hADSCs (red) were injected into the contralateral hemisphere of the tumor. hADSCs displayed long-range directional migration and infiltration toward GBM tumors in the contralateral brain (*B*–*E*), but no migration was observed in the control group (*F* and *G*). Green indicates PKH67 labeled GBM cells, red indicates Dil-labeled hADSCs, blue indicates DAPI staining of cell nuclei, and white arrows indicate the colocalization of hADSCs and GBM cells. (Scale bars: 1 mm.)

the tumor brain, Dil-labeled hADSCs mostly occurred at the tumor margin (Fig. 4*D*). Interestingly, hADSCs colocalized with the infiltrating GBM cells at a distance from the main tumor mass (Fig. 4*E*). Our in vivo antitumor efficacy study also revealed obvious migration of NPs/pTRAIL-engineered hADSCs within 10 d, with appreciable TRAIL secretion after intratumoral (i.t.) administration (Fig. 6*A*); migrating hADSCs remained at the border of the tumor, where it interfaced with normal tissue at day 10. Thus, hADSCs demonstrated a robust migratory capacity and glioma tropism in vivo and exhibited an ability to "seek" infiltrating glioma cells, which is significant for GBM treatment. In contrast, when hADSCs were injected through a tail vein, no hADSCs were detected in the brain (Fig. S7), suggesting local delivery within the brain is required for effective tumor targeting.

Effects of NPs/pTRAIL-hADSCs on Tumor Growth and Survival of Patient-Derived Adult Glioblastoma Orthotropic Xenograft Models. A change in body weight was recorded at 15 d after i.t. injection of hADSCs because the mice in the PBS group died on day 15. At the same time point, there was less weight loss in the NPs/pTRAIL-hADSCs group than in any of the three control groups (Fig. 5*B*).

We wished to ascertain whether the potent induction of apoptosis associated with NPs/pTRAIL-hADSC therapy would translate into inhibition of tumor growth in vivo. Maximal tumor surface areas were determined from patient-derived GBM-bearing brains harvested from mice euthanized 10 d after treatment with NPs/pTRAIL-hADSCs (Fig. 5 *C* and *D*). The average maximal tumor areas in NPs/pCDNA-hADSCs, naïve hADSCs, and PBS solution-treated animals were 2.60 ± 0.59 mm^2, 2.65 ± 0.44 mm^2, and 2.68 ± 0.32 mm^2, respectively, compared with 0.92 ± 0.60 mm^2 in NPs/pTRAIL-hADSC–treated brains ($P < 0.01$, NPs/pTRAIL-hADSCs vs. other groups; Fig. 5 *C* and *D*).

The survival of mice treated with NPs/pTRAIL-hADSCs was significantly longer than that of controls treated with NPs/pCDNA-hADSCs, hADSCs, or PBS solution (Fig. 5*E*). There were no detectable differences in survival among control groups treated with NPs/pCDNA-hADSCs, hADSCs, or PBS solution. Statistical analysis revealed that the effects of NPs/pTRAIL-hADSCs were significantly different from those of controls ($P = 0.0146$, NPs/pTRAIL-hADSCs vs. NPs/pCDNA-hADSCs; $P = 0.0069$, NPs/pTRAIL-hADSCs vs. hADSCs; $P = 0.0047$, NPs/pTRAIL-hADSCs vs. PBS solution; Table S1). Repetitive i.t. injection with NPs/pTRAIL-hADSCs in patient-derived GBM mice further prolonged survival compared with a single i.t. injection (Fig. 5*F*). These data indicate that treatment with NPs/pTRAIL-hADSCs has a strong antitumor effect and that repetitive treatment with NPs/pTRAIL-hADSCs could significantly enhance anti-GBM efficacy ($P = 0.0254$, repetitive injection of NPs/pTRAIL-hADSCs vs. single treatment; Table S1).

In Vivo Expression of TRAIL and Induction of Apoptosis in Patient-Derived GBM Orthotropic Xenograft Models by Inoculated NPs/pTRAIL-Engineered hADSCs. We quantitatively measured the levels of TRAIL protein expression in vivo at day 10 after treatment with NPs/pTRAIL-hADSCs. Tissues prepared from mice displayed strong immunochemical staining for TRAIL within inoculated tumors and on the border of the tumor mass, indicating the presence of TRAIL-expressing hADSCs even >10 d after implantation (Fig. 6*A*).

To evaluate the ability of NPs/pTRAIL-hADSCs to induce apoptosis in established intracranial gliomas, we performed TUNEL staining on tumor-bearing brain sections from animals that underwent distinct treatments. NPs/pTRAIL-hADSC–treated tumors were nearly completely apoptotic (Fig. 6*B*), indicating that TRAIL expression from transplanted hADSCs induced rapid

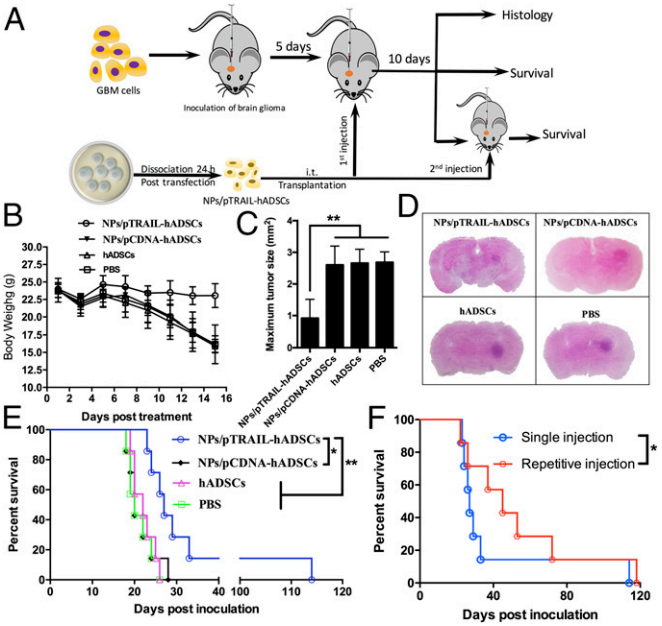

Fig. 5. TRAIL-overexpressing hADSCs inhibited GBM growth and extended survival in a mouse GBM model in vivo. (*A*) Schematic of experimental design. NPs/pTRAIL-engineered hADSCs, hADSCs (3×10^5 cells), or PBS solution were administered i.t. to glioma-bearing mice at day 5 after glioma (7×10^5 cells) inoculation. For the repetitive injection group, the second dose of NPs/pTRAIL-engineered hADSCs was given at day 10 after the first dose. (*B*) Changes in body weight of mice as a function of time in intracranial glioma-bearing mice ($n = 7$). (*C*) Tumor size was determined by histologic analysis at day 15 after tumor inoculation ($n = 3$ per treatment group; $^{**}P < 0.01$). (*D*) Representative photographs of H&E staining from each group show tumor growth. (Magnification, 1×.) (*E*) Survival curve of intracranial glioma-bearing mice after treatment with a single dose of NPs/pTRAIL-engineered hADSCs, hADSCs (3×10^5 cells), or PBS solution. (*F*) Survival after treatment with repetitive doses of NPs/pTRAIL-engineered hADSCs. For *E* and *F*, survival analysis was conducted by a log-rank test based on the Kaplan–Meier method ($n = 7$ per treatment group; $^{*}P < 0.05$ and $^{**}P < 0.01$).

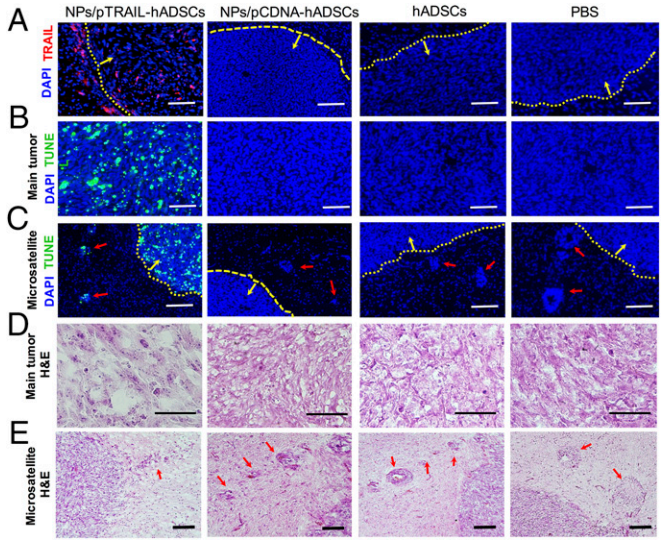

Fig. 6. TRAIL-overexpressing hADSCs induced GBM apoptosis and reduced tumor mass and the occurrence of microsatellites in a mouse GBM xenograft model. Mice were treated with NPs/pTRAIL-hADSCs or controls (NPs/pCDNA-hADSCs, unmodified hADSCs, or PBS solution control) at day 5 after glioma (7×10^5 cells) inoculation. Brain tissues were harvested 10 d after treatment for histologic examination. (*A*) Positive staining for TRAIL (red) was evidenced in the tumor mass and around the tumor border, indicating the survival of TRAIL-overexpressing hADSCs. No TRAIL expression was detected in controls. (*B* and *C*) TUNEL staining confirmed TRAIL-hADSCs induced specific apoptosis in GBM tumor mass (*B*) and in microsatellites (*C*), but not in controls. Red indicates TRAIL, blue indicates cell nuclei, green indicates TUNEL, red arrow indicates microsatellite outgrowing from primary tumor mass into adjacent normal brain, yellow arrow points to inside tumor mass, and dotted yellow line indicates tumor edge. (*D*) Hematoxylin and eosin (H&E) staining of tumor mass showed disrupted tumor morphology and markedly reduced tumor density in the NPs/pTRAIL-hADSC–treated group versus control groups. (*E*) H&E staining of tumor/normal brain interface. Fewer microsatellites occurred in NPs/pTRAIL-hADSC–treated group than that in the control groups. Red arrow indicates microsatellite outgrowth from the primary tumor mass into adjacent normal brain. (Scale bars, 100 μm.)

tumor cell death in vivo. There was negligible apoptotic activity in tumors treated with NPs/pCDNA-hADSCs, hADSCs, or PBS solution. Importantly, apoptotic cells were detected not only in the main tumor mass but also near invading tumor microsatellites (Fig. 6*C*), indicating that NPs/pTRAIL-hADSCs sought and migrated through tumor outgrowths from the primary tumor site into adjacent normal tissue and induced tumor-cell apoptosis in infiltrating tumor islands. At the same time, apoptosis was confined to the main tumor mass and tumor microsatellites, with no involvement of normal brain parenchyma.

Tumor slices stained with H&E were analyzed via optical microscopy. Qualitatively, the necrotic areas in NPs/pTRAIL-hADSC–treated tumors were larger than in other groups (Fig. 6*D*). Fewer microsatellite outgrowths occurred in NPs/pTRAIL-hADSC–treated tumors than in tumors treated with NPs/pCDNA-hADSCs, hADSCs, or PBS solution (Fig. 6*E*).

Discussion

Current treatment for GBM fails to address its highly infiltrative nature; treatment often leaves behind microscopic neoplastic satellites, resulting in eventual tumor recurrence. Tracking and eliminating the tumor microsatellites and infiltrating gliomas cells is therefore of utmost importance in GBM treatment. Although stem cells have been previously used as drug-delivery vehicles for potential cancer therapy, the strategy reported here is unique in multiple aspects. First, our method replaces viral vectors (27–29) with nonviral polymeric nanoparticles for overexpressing therapeutic factors in stem cells, which is potentially safer, easy to scale up, and more attractive for broad clinical translations. Second, to overcome the ethical concerns and cell scarcity limitations associated with NSCs (6, 7), here we have demonstrated the efficacy of adipose-derived stem cells as an abundant and easily accessible autologous cell source for targeting infiltrating GBM and microsatellites over long distances in vivo. Third, membrane-bound TRAIL was chosen as a therapeutic agent overexpressed by polymeric nanoparticles, which markedly augment receptor clustering and apoptosis stimulation in cancer cells (30, 31). Last, patient-derived GBM xenograft cells were used rather than immortalized cell lines, which have been shown to better at preserving tumor phenotype and predicting clinically relevant outcomes (26).

As we demonstrated here, hADSCs extensively home to brain tumors and track infiltrating tumor cells and microsatellite outgrowths from the main solid tumor mass. These behaviors are particularly relevant because current treatment approaches cannot identify or treat microsatellites directly, ultimately leading to recurrence. The other attractive aspect of this platform is the ease of extracting, culturing, and obtaining hADSCs for autologous stem-cell therapy. A key obstacle of stem cell-based gene therapy is the lack of safe and effective gene delivery systems. Viral vectors are the current gold standard for achieving high gene delivery efficiency into various human stem cells (27–29), but the broad clinical applications are limited by potential immune responses and unintended genomic integration events (21, 22). Here, we report a safe and efficient method for transducing hADSCs with a full-length TRAIL using hydrolysable polymeric nanoparticles. Our results showed that polymeric nanoparticle-mediated transfection led to robust up-regulation of membrane-bound TRAIL in hADSCs, and that TRAIL-expressing hADSCs induced tumor-specific apoptosis. Despite extensive preclinical documentation of the antitumor potential of TRAIL, studies in patients with cancer have demonstrated little efficacy. Potential reasons for the lack of clinical efficacy may include insufficient tumor exposure (16, 17) and/or weak engagement of the extrinsic pathway (10, 13). We have chosen membrane display of TRAIL, which could more faithfully mimic the endogenous ligand, and markedly augment receptor clustering and apoptosis stimulation in cancer cells (30, 31). Indeed, our results showed polymeric nanoparticles-induced TRAIL overexpressing led to effective targeting of intracranial brain tumor and microsatellite tumor cells in a patient-derived glioblastoma orthotopic xenograft models, paving the way for clinical translation of this innovative therapeutic approach.

For targeting tumor in vivo using cell-based drug vehicles, it would be important to determine the optimal route for cell delivery. We have compared systemic delivery route vs. intracranial local delivery, and examined the impacts on the efficacy of hADSCs to migrate toward GBM patient-derived tumor xenograft (PDTX) cells in the brain. Intracranial injection of TRAIL-overexpressing hADSCs demonstrated strong tumor tropism with long-range migration toward GBM and colocalized with tumor microsatellites (Fig. 4 *D* and *E*). In contrast, when hADSCs were injected i.v. through a tail vein, no hADSCs were detected in the brain (Fig. S7), suggesting local delivery within the brain is required for effective tumor targeting. Such a lack of tumor tropism with the use of systemic delivery is likely a result of the blood-brain barrier. Consistent with our finding, previous studies using NSCs for targeting brain tumors have also chosen a local delivery route inside the brain to achieve targeting efficacy (1–5). Although the method reported here is efficient only through intracranial delivery, but not systemic delivery, it is very compatible with the current modalities of cancer therapies and can be combined with current clinical treatment plan without additional surgery. For patients with GBM, surgical tumor resection is always the first intervention to remove the

bulk solid tumor, which exposes a cavity for the injection of therapeutic cells/agents. Nonviral engineered hADSCs can be injected during the same surgery of bulk tumor removal to target and eradicate the infiltrating tumor microsatellites that cannot be surgically removed. The promise of such an approach has been demonstrated recently by injecting viral engineered NSCs and bone marrow-derived MSCs into brain cavity after bulk tumor resection (1, 2). Together, our results suggest that local intracranial delivery of nonviral modified hADSCs is more effective than systemic delivery for targeting infiltrating microsatellite cells to prevent brain tumor recurrence. i.t. injection of TRAIL-overexpressing hADSCs not only significantly inhibited main GBM growth and extended survival, but also reduced the occurrence of microsatellites. Furthermore, repetitive injection of TRAIL-overexpressing hADSCs significantly prolonged animal survival compared with single injection of these cells. As such, our findings add credence to the elimination of disseminated microsatellites or residual neoplastic foci in GBM patients in a seek-and-destroy manner by engrafting nanoparticle-induced TRAIL-expressing autologous stem cells.

Materials and Methods

All reagents and additional procedures used in this study, including primary cell isolation and culture and cell characterization, polymeric nanoparticle synthesis and characterization, optimization of transfection formulation, immunocytochemical and immunohistochemical assays, qRT-PCR, Western blotting, cell viability analysis, in vitro coculture and apoptosis analysis, flow cytometry, and statistical analyses are described in *SI Materials and Methods*. All animal procedures were performed with approval from the appropriate animal care and use committee (Stanford University Administrative Panel on Laboratory Animal Care and Use Committee). All procedures adhered to the US National Institutes of Health Guide for the Care and Use of Laboratory Animals.

ACKNOWLEDGMENTS. This work was supported by an Alliance for Cancer Gene Therapy Young Investigator Award Grant (to F.Y.), a Stanford School of Medicine Dean's postdoctoral fellowship (X.J.), a Child Health Research Institute Grant and postdoctoral fellowship (X.J.), National Institutes of Health Grants R01DE024772 (to F.Y.) and K08 NS075144 (to G.A.G), National Science Foundation CAREER Award CBET-1351289 (to F.Y.), California Institute for Regenerative Medicine Tools and Technologies Award RT3-07804 (to F.Y.), a Stanford Chem-H Institute Biomaterials Seed Grant (to F.Y.), the Stanford Bio-X Interdisciplinary Initiative Program (F.Y.), a Stanford Child Health Research Institute Faculty Scholar Award (to F.Y.), and the Arline and Pete Harman Endowed Faculty Scholar Stanford Child Health Research Institute (G.A.G.).

1. Kauer TM, Figueiredo J-L, Hingtgen S, Shah K (2011) Encapsulated therapeutic stem cells implanted in the tumor resection cavity induce cell death in gliomas. *Nat Neurosci* 15(2):197–204.
2. Redjal N, Zhu Y, Shah K (2015) Combination of systemic chemotherapy with local stem cell delivered S-TRAIL in resected brain tumors. *Stem Cells* 33(1):101–110.
3. Bagci-Onder T, Du W, Figueiredo J-L, Martinez-Quintanilla J, Shah K (2015) Targeting breast to brain metastatic tumours with death receptor ligand expressing therapeutic stem cells. *Brain* 138(pt 6):1710–1721.
4. Aboody KS, et al. (2000) Neural stem cells display extensive tropism for pathology in adult brain: Evidence from intracranial gliomas. *Proc Natl Acad Sci USA* 97(23): 12846–12851.
5. Aboody KS, et al. (2013) Neural stem cell–mediated enzyme/prodrug therapy for glioma: Preclinical studies. *Sci Transl Med* 5(184):184ra159.
6. Arsenijevic Y, et al. (2001) Isolation of multipotent neural precursors residing in the cortex of the adult human brain. *Exp Neurol* 170(1):48–62.
7. Yu JJ, et al. (2006) Immunomodulatory neural stem cells for brain tumour therapy. *Expert Opin Biol Ther* 6(12):1255–1262.
8. Sasportas LS, et al. (2009) Assessment of therapeutic efficacy and fate of engineered human mesenchymal stem cells for cancer therapy. *Proc Natl Acad Sci USA* 106(12): 4822–4827.
9. Vilalta M, et al. (2008) Biodistribution, long-term survival, and safety of human adipose tissue-derived mesenchymal stem cells transplanted in nude mice by high sensitivity non-invasive bioluminescence imaging. *Stem Cells Dev* 17(5):993–1003.
10. Pacioni S, et al. (2015) Mesenchymal stromal cells loaded with paclitaxel induce cytotoxic damage in glioblastoma brain xenografts. *Stem Cell Res Ther* 6(1):194.
11. Bonomi A, et al. (2015) Human amniotic mesenchymal stromal cells (hAMSCs) as potential vehicles for drug delivery in cancer therapy: An in vitro study. *Stem Cell Res Ther* 6(1):155.
12. Pessina A, et al. (2011) Mesenchymal stromal cells primed with paclitaxel provide a new approach for cancer therapy. *PLoS One* 6(12):e28321.
13. Levy O, et al. (2016) A prodrug-doped cellular Trojan Horse for the potential treatment of prostate cancer. *Biomaterials* 91:140–150.
14. Levy O, et al. (2013) mRNA-engineered mesenchymal stem cells for targeted delivery of interleukin-10 to sites of inflammation. *Blood* 122(14):e23–e32.
15. Wang S, El-Deiry WS (2003) TRAIL and apoptosis induction by TNF-family death receptors. *Oncogene* 22(53):8628–8633.
16. Wang S (2008) The promise of cancer therapeutics targeting the TNF-related apoptosis-inducing ligand and TRAIL receptor pathway. *Oncogene* 27(48):6207–6215.
17. Herbst RS, et al. (2010) Phase I dose-escalation study of recombinant human Apo2L/TRAIL, a dual proapoptotic receptor agonist, in patients with advanced cancer. *J Clin Oncol* 28(17):2839–2846.
18. Kelley SK, et al. (2001) Preclinical studies to predict the disposition of Apo2L/tumor necrosis factor-related apoptosis-inducing ligand in humans: Characterization of in vivo efficacy, pharmacokinetics, and safety. *J Pharmacol Exp Ther* 299(1):31–38.
19. Soria JC, et al. (2011) Randomized phase II study of dulanermin in combination with paclitaxel, carboplatin, and bevacizumab in advanced non–small-cell lung cancer. *J Clin Oncol* 29(33):4442–51.
20. Ashkenazi A, Holland P, Eckhardt SG (2008) Ligand-based targeting of apoptosis in cancer: The potential of recombinant human apoptosis ligand 2/Tumor necrosis factor-related apoptosis-inducing ligand (rhApo2L/TRAIL). *J Clin Oncol* 26(21):3621–3630.
21. Brown BD, et al. (2007) In vivo administration of lentiviral vectors triggers a type I interferon response that restricts hepatocyte gene transfer and promotes vector clearance. *Blood* 109(7):2797–2805.
22. Nayak S, Herzog RW (2010) Progress and prospects: Immune responses to viral vectors. *Gene Ther* 17(3):295–304.
23. Yang F, et al. (2009) Gene delivery to human adult and embryonic cell-derived stem cells using biodegradable nanoparticulate polymeric vectors. *Gene Ther* 16(4): 533–546.
24. Yang F, et al. (2010) Genetic engineering of human stem cells for enhanced angiogenesis using biodegradable polymeric nanoparticles. *Proc Natl Acad Sci USA* 107(8): 3317–3322.
25. Kim SM, et al. (2008) Gene therapy using TRAIL-secreting human umbilical cord blood-derived mesenchymal stem cells against intracranial glioma. *Cancer Res* 68(23): 9614–9623.
26. Hidalgo M, et al. (2014) Patient-derived xenograft models: An emerging platform for translational cancer research. *Cancer Discov* 4(9):998–1013.
27. Ehtesham M, et al. (2002) Induction of glioblastoma apoptosis using neural stem cell-mediated delivery of tumor necrosis factor-related apoptosis-inducing ligand. *Cancer Res* 62(24):7170–7174.
28. Grisendi G, et al. (2010) Adipose-derived mesenchymal stem cells as stable source of tumor necrosis factor-related apoptosis-inducing ligand delivery for cancer therapy. *Cancer Res* 70(9):3718–3729.
29. Loebinger MR, Eddaoudi A, Davies D, Janes SM (2009) Mesenchymal stem cell delivery of TRAIL can eliminate metastatic cancer. *Cancer Res* 69(10):4134–4142.
30. Mitchell MJ, Wayne E, Rana K, Schaffer CB, King MR (2014) TRAIL-coated leukocytes that kill cancer cells in the circulation. *Proc Natl Acad Sci USA* 111(3):930–935.
31. Nair PM, et al. (2015) Enhancing the antitumor efficacy of a cell-surface death ligand by covalent membrane display. *Proc Natl Acad Sci USA* 112(18):5679–5684.
32. Keir ST, Friedman HS, Reardon DA, Bigner DD, Gray LA (2013) Mibefradil, a novel therapy for glioblastoma multiforme: Cell cycle synchronization and interlaced therapy in a murine model. *J Neurooncol* 111(2):97–102.